INTERFACIAL STABILITY IN VERTICAL SWIRLING ANNULAR TWO-PHASE FLOW

Li Liu, Bofeng Bai*
State Key Laboratory of Multiphase Flow in Power Engineering
Xi'an Jiaotong University, Xi'an 710049, China
liulide@stu.xjtu.edu.cn; bfbai@mail.xjtu.edu.cn

ABSTRACT

The linear stability of liquid film flowing upward the inner surface of vertical cylinder under the action of the swirling gas core flow is investigated taking exactly the centrifugal force and curvature of the cylinder into account. Swirl has been considered by superposing a circular movement on the annular flow. The theoretical model of the stability of interface to small perturbation is established by analyzing the normal force balance condition at the wavy interface. The characteristic equation is solved and the stability criterion is obtained. The stability characteristics of neutral, growing and damped modes are presented showing the influences of swirl intensity, relative motion of gas-liquid flow, and the surface tension force. The modeling results indicate that the swirling of the gas phase stabilizes the film flow while the curvature of the cylinder destabilizes it. For strong swirling annular flow, it is found that there is a small influence of surface tension on the stability of interface because the stabilizing centrifugal force is dominant on this condition. The neutral wavelength is found to be very sensitive to the values of swirl intensity and cylinder radius when gas-liquid relative movement is small. However, when gas flow rate is large enough, there is no significant difference in its value.

KEYWORDS
Swirling annular two-phase flow, interfacial waves, K-H instability, stability criterion

1. INTRODUCTION

The swirling annular two-phase flow is encountered in a variety of industry applications, such as swirl separators for gas-liquid separation, vortex tools for liquid drainage in wet-gas wells and heat exchangers for flow-boiling heat transfer [1-6]. This flow is characterized by the presence of a thin liquid film adjacent to the wall and a continuous rotating gas core in the centre. With the strong shear action of gas stream, the interface between the phases is not smooth but covered with a complex pattern of waves. An understanding of the interfacial stability is considerable practical importance for the study of mass, momentum and heat transfer between the phases, since the unstable interface directly leads to droplet entrainment. The entrained droplets finally exert in many important parameters of both flow and heat transfer processes, resulting in reduced separation efficiency in separators and deteriorated heat transfer in heat exchangers. To analyze and simulate swirling annular two-phase flows, it is highly desirable to obtain a general model based upon physical modeling which can provide a basis for the understanding of the interfacial phenomenon and lay a foundation for the further study of droplet entrainment.

In the annular/stratified regime of gas-liquid flows, the combination of normal stresses exerted by gas and liquid phases and surface tension stress makes the interface wavy. Fig. 1 shows the streamlines over a wavy interface and the normal forces acting on the interface [7]. If the gas velocity flowing along the interface is large enough, an imbalance between the pressure force acting on the wave crest and surface tension can occur. As suggested by [8, 9], this force imbalance, known as a K-H instability, is the primary

mechanism by which interfacial wave growth and droplet entrainment occur. [10] concluded that large growth rates can occur when the wavelength is in the K-H instability range. For the entrained droplet, the assumption of [10] also proposed that the droplet size is directly proportional to the wavelength that produced it. [11] point out that the wavelength making the greatest contribution to the rate of droplet entrainment scales as the film height in thin liquid film, and the critical wavelength is the most key parameter for entrainment prediction, since the volume of liquid detaching from the surface is directly proportional to this wavelength. [12] suggested that the K-H instability would cause any wavy disturbances on the interface of stratified flow to grow in amplitude and such wave would break to form droplets even with small shear velocities when the liquid flow is laminar. In the stratified flow, [13] developed a criterion for the wave amplitude required to destabilize the wave at a certain wavelength. This model was then extended to predict the onset of entrainment and the transition of flow patterns. More recently, [14, 15] conducted a stability analysis to calculate the wavelength and velocity of the unstable waves in gas-liquid annular flow. The critical interfacial conditions that lead to droplet entrainment were then obtained. From the discussion above, it is clear that the K-H instability mechanism is very important in wave-propagation phenomenon and the interfacial waves play a crucial role in the transport behavior of two-phase flows.

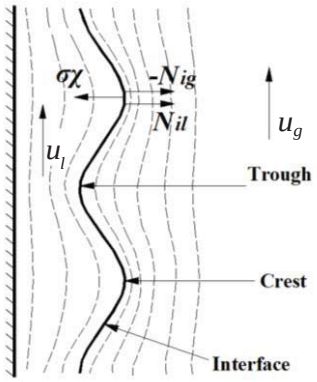

Figure 1. Stresses and streamlines in stratified/annular two-phase flow with a wavy interface.

Although the liquid film developed on the cylinders have received a reasonable amount of attention in the literatures, most of the studies are performed mainly on stratified/annular flows without rotation, the exploration on the stability problem of liquid film in swirling flow conditions is limited and the existing researches are mostly focused on the stability of a liquid layer flowing inside a rotating cylinder [16-21]. For the two-phase swirling flows, [22] proposed a simple model to study the effect of the swirl intensity and gas/liquid dynamic pressure ratio on the stability of a swiled liquid film entrained by a fast gas stream. [23] presented a linear model to describe the instability behavior of annular, swirling, inviscid liquid sheet subject to inner and outer gas flows of differing velocities. However, the general stability criteria were not able to obtain in their models due to the complicated characteristic equations.

In this paper, the interfacial stability of liquid film in swirling annular flow is investigated based on the two-fluid flow model. The three-dimensional gas flow in a stationary cylinder is firstly decomposed into two normal modes, the annular flow inside a cylinder superposes a circular movement in a plane polar. In both cases, gas and liquid phases are assumed to be inviscid and separated by an interface on which waves move with a certain velocity. By considering the action of two phases separately, the normal stress exerted by each phase on the interface is evaluated. Specially, the centrifugal force induced by swirl is treated as an additional normal stress in this analysis. The theoretical model of the stability of interface to small perturbation is then established by analyzing the normal force balance condition at the interface. The characteristic equation is solved and the stability criterion is obtained. The stability characteristics of neutral, growing and damped modes are presented showing the influences of swirl intensity, relative motion of gas-liquid flow, and the surface tension force. The results will help us gain a qualitative

understanding of the disturbance spectrum of the film flow and provide a basis for the further study of droplet entrainment in the swirling annular two-phase flow.

2. THE MATHEMATICAL MODEL

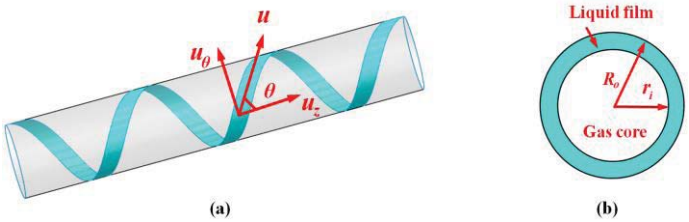

Figure 2. Geometric configuration of the Swirling annular two-phase flow.

The swirling annular flow insider a cylinder is depicted in Fig. 2. We make the following preliminary assumptions regarding the basic two-phase flow. 1) The gas and liquid flow are immiscible and there is no mass transfer across the interface; 2) the flow is steady in time, fully developed in the axial direction and is axially symmetric. Cylindrical coordinates (r, θ, z) and plane polar coordinates (r, θ) moving with waves are used for annular flow and circular movement, where r, θ, z denote the radial, azimuthal and axial directions, respectively. The cylinder radius is R_o and the radial position of the interface is r_i. The approximate analytical method presented by [7] is adopted as a basis for the present study.

2.1. Interfacial waves

According to the K-H instability, the study of the stability of an interface to small perturbation $\hat{y}$ is assumed that the slope of the interface is everywhere small [7]. The shape of the wavy interface is approximated by a cosine wave as

$$y = \hat{y}\cos k(s - ct) \tag{1}$$

where y, $\hat{y}$, s and k are the distance from the wall, disturbance amplitude, streamwise direction and wavenumber ($k=2\pi/\lambda$), respectively. If the wave velocity c is complex ($c=c_R+ic_I$), Eq. (1) becomes

$$y = \hat{y}\cos k(s - c_R t)\exp(kc_I t) \tag{2}$$

The physical significance of c_R is the propagation velocity of the disturbance, while c_I represents the growth rate. Eq. (2) shows that when $c_I>0$, the waves amplitude increases exponentially with time and the flow is untable; when $c_I<0$, the amplitude decreases exponentially with time and the flow is stable; when $c_I=0$, the amplitude remains constant, which is defined as the neutral stability condition.

2.2. Gas core analysis

2.1.1. Annular flow

In cylindrical coordinates, the equations of continuity and motion for gas phase in axisymmetric annular flow can be expressed as

$$\begin{aligned}
&\frac{1}{r}\frac{\partial}{\partial r}(ru_r) + \frac{\partial u_z}{\partial z} = 0 \\
&u_r\frac{\partial u_r}{\partial r} + u_z\frac{\partial u_r}{\partial z} = -\frac{1}{\rho_g}\frac{\partial p}{\partial r} + v_g\left[\frac{1}{r}\frac{\partial}{\partial r}\left(r\frac{\partial u_r}{\partial r}\right) + \frac{\partial^2 u_r}{\partial z^2} - \frac{u_r}{r^2}\right] \\
&u_r\frac{\partial u_z}{\partial r} + u_z\frac{\partial u_z}{\partial z} = -\frac{1}{\rho_g}\frac{\partial p}{\partial z} + v_g\left[\frac{1}{r}\frac{\partial}{\partial r}\left(r\frac{\partial u_z}{\partial r}\right) + \frac{\partial^2 u_z}{\partial z^2}\right]
\end{aligned} \tag{3}$$

where *p* is the pressure, respectively. The effect of gravity force is not considered since the instability analysis is only performed in the radial direction.

The disturbance to the interface is accompanied by velocity and pressure fluctuations in the base flow, by introducing the stream function ψ , the respective velocity components can be expressed as

$$u_z = \partial\psi / r\partial r \quad , \; u_r = -\partial\psi / r\partial z \tag{4}$$

The stream function and pressure are expressed in terms of real and imaginary components representing a steady solution and a perturbation induced at the wave interface as

$$\psi = \bar{\psi}(r) + \hat{\psi}(r)e^{ikz}, \qquad p = \bar{p}(z) + \hat{p}(r)e^{ikz} \tag{5}$$

Substituting Eqs. (4) and (5) into Eq (3), eliminating the steady-state solution and neglecting second order terms, the equations governing disturbance are obtained.

$$\bar{u}_z \frac{D\hat{\psi}}{r} - D\bar{u}_z \frac{\hat{\psi}}{r} = -\frac{\hat{p}}{\rho_g} + \frac{v_g}{ik}\left(\frac{D^3\hat{\psi}}{r} - k^2 \frac{D\hat{\psi}}{r} \right) \tag{6}$$

$$k^2 \bar{u}_z \frac{\hat{\psi}}{r} = -\frac{D\hat{p}}{\rho_g} - ikv_g \left(\frac{D^2\hat{\psi}}{r} - \frac{D\hat{\psi}}{r^2} - k^2 \frac{\hat{\psi}}{r} \right) \tag{7}$$

where $D = \partial / \partial r$.

Eliminating the perturbed pressure $\hat{p}$ from above two equations and assuming the gas flow is inviscid yields the following Orr-Sommerfeld equation.

$$D^2\hat{\psi} - D\hat{\psi}/r - k^2\hat{\psi} = 0 \tag{8}$$

where $D^2 = \partial^2 / \partial r^2$.

The general solution for $\hat{\psi}$ is given in terms of the first-order modified Bessel functions of the first and second kinds, I_1 and K_1, as

$$\hat{\psi} = ArI_1(kr) + BrK_1(kr) \tag{9}$$

where the constants *A* and *B* can be determined according to the following boundary conditions.

The radial velocity component can be calculated from Eq. (4) and Eq. (9) as

$$\hat{u}_r = -\partial\hat{\psi} / r\partial z = -ik\left[ArI_1(kr) + BrK_1(kr) \right] e^{ikz} \tag{10}$$

Since the gas core in annular flow is assumed to be axisymmetric, the boundary condition of radial velocity component along the cylinder axis *r*=0 is given as

$$\hat{u}_r = 0 \tag{11}$$

Assuming that the flow is uniform and the axial velocity at all points, including interface, is the same. Then the boundary condition of radial velocity component at the perturbed interface r_i can be approximated according to the uniform flow in axial direction as

$$\hat{u}_r = \left(\bar{u}_z - c_z \right) \partial r_i / \partial z \tag{12}$$

where

$$r_i = \left(R_o - \bar{\delta} \right) + \hat{\delta} e^{ikz} \tag{13}$$

Then

$$\hat{u}_r = ik\hat{\delta}\left(\bar{u}_z - c_z \right) e^{ikz} \tag{14}$$

where $\bar{\delta}$, $\hat{\delta}$, $\bar{u}_z$ and c_z are the average and perturbed film thickness, average axial velocity and axial wave velocity, respectively.

Taking the above boundary conditions into account, the constants $A = -\hat{\delta}(\bar{u}_z - c_z) / I_1(k\bar{r}_i)$ and $B = 0$, then the final expression for the perturbation of the stream function is obtained

$$\hat{\psi}(r) = -\hat{\delta}(\bar{u}_z - c_z)\frac{rI_1(kr)}{I_1(k\bar{r}_i)} \tag{15}$$

where $\bar{r}_i = R_o - \bar{\delta}$ is the mean radial position of the interface.

Based on Eq. (15), the amplitude of the perturbed pressure can be derived from the integration of Eq. (7), which is related to the average axial velocity $\bar{u}_z$ as

$$\hat{p}_g = \rho_g k\hat{\delta}\left(\bar{u}_z - c_z\right)^2 \frac{I_0(kr)-1}{I_1(k\bar{r}_i)} \tag{16}$$

where I_0 is the zero-order modified Bessel function of first kind.

The normal stress perturbation $\left(\hat{N}_{ig}\right)_1$ exerted by gas phase on the interface $r = r_i$ equals to the magnitude of the perturbed pressure $\hat{p}_g$ and acts outward and perpendicular to the interface, can be expressed as

$$\left(\hat{N}_{ig}\right)_1 = -\hat{p}_g = -\rho_g k\hat{\delta}\left(\bar{u}_z - c_z\right)^2 \frac{I_0(k\bar{r}_i)-1}{I_1(k\bar{r}_i)} \tag{17}$$

Fig. 3 shows how the ratio of $\left[I_0\left(k\bar{r}_i\right)-1\right]/I_1\left(k\bar{r}_i\right)$ changes with the variable $k\bar{r}_i$.

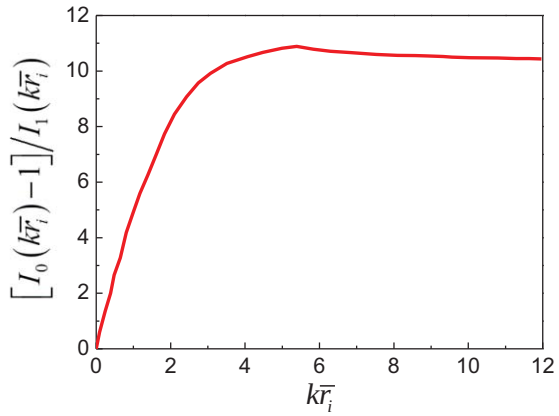

Figure 3. Dependence of the value of $\left[I_0\left(k\bar{r}_i\right)-1\right]/I_1\left(k\bar{r}_i\right)$ variation upon $k\bar{r}_i$.

Generally, the wavelength in annular flow is in order of 0.1~1 millimeter [24], for very large radius to wavelength ratios $k\bar{r}_i \geq 3$, the value of $\left[I_0(k\bar{r}_i)-1\right]/I_1(k\bar{r}_i)$ tend to unity. Then the Eq. (17) reduces to

$$\left(\hat{N}_{ig}\right)_1 = -k\hat{\delta}\rho_g\left(\bar{u}_z - c_z\right)^2 \tag{18}$$

2.1.1. Circular movement

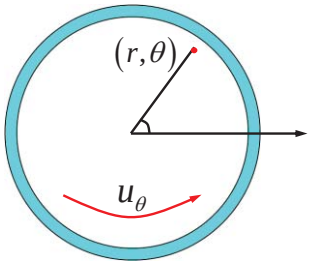

Figure 4. Circular movement of gas core in plane polar coordinates.

In plane polar coordinates (Fig. 4), the equations of motion and continuity for gas phase in circular movement can be expressed as

$$\begin{aligned}
&\frac{1}{r}\frac{\partial}{\partial r}\left(ru_r\right)+\frac{1}{r}\frac{\partial u_\theta}{\partial \theta}=0\\
&u_r\frac{\partial u_r}{\partial r}+\frac{u_\theta}{r}\frac{\partial u_r}{\partial \theta}-\frac{u_\theta^2}{r}=-\frac{1}{\rho_g}\frac{\partial p}{\partial r}+\nu_g\left[\nabla^2 u_r-\frac{u_r}{r^2}-\frac{2}{r^2}\frac{\partial u_\theta}{\partial \theta}\right]\\
&u_r\frac{\partial u_\theta}{\partial r}+\frac{u_\theta}{r}\frac{\partial u_\theta}{\partial \theta}+\frac{u_r u_\theta}{r}=-\frac{1}{\rho_g}\frac{\partial p}{r\partial \theta}+\nu_g\left[\nabla^2 u_\theta-\frac{u_\theta}{r^2}+\frac{2}{r^2}\frac{\partial u_r}{\partial \theta}\right]
\end{aligned} \tag{19}$$

where $\nabla^2=\frac{\partial^2}{\partial r^2}+\frac{1}{r}\frac{\partial}{\partial r}+\frac{1}{r^2}\frac{\partial^2}{\partial \theta^2}$.

By introducing stream function ψ and using a similar analysis procedure as above (the details of analysis are shown in Appendix A), the amplitude of the perturbed pressure can be derived. Specially, since the gas phase is assumed to be inviscid, the model of a potential vortex flow is adopted for circular movement in this case, i.e $u_{g,\theta}=C/r$. Thus, we obtain the perturbed normal stress exerted by the gas core in circular movement on the interface ($r=\bar{r}_i$)

$$\left(\hat{N}_{ig}\right)_2=-\left[\rho_g\hat{\delta}m\frac{\left(\bar{u}_\theta-c_\theta\right)^2}{\bar{r}_i}\frac{2m}{\sqrt{1+4m^2}-3}+\rho_g\hat{\delta}\frac{\bar{u}_\theta^2}{\bar{r}_i}\frac{\sqrt{1+4m^2}+1}{\sqrt{1+4m^2}-3}\right] \tag{20}$$

where m and $\bar{u}_{g,\theta}$ are the azimuthal wavenumber (nondimensional) and the average azimuthal velocity at the interface, respectively.

Fig. 5(a) and (b) shows how the ratios of $2m\Big/\left(\sqrt{1+4m^2}-3\right)$ and $\left(\sqrt{1+4m^2}+1\right)\Big/\left(\sqrt{1+4m^2}-3\right)$ change with the azimuthal wavenumber *m*. For very large radius to wavelength ratios, the wavenumber *m* is large enough that the values of $2m\Big/\left(\sqrt{1+4m^2}-3\right)$ and $\left(\sqrt{1+4m^2}+1\right)\Big/\left(\sqrt{1+4m^2}-3\right)$ tend to unity. Under this condition, the Eq. (20) can be simplified to

$$\left(\hat{N}_{ig}\right)_2=-\left[\rho_g\hat{\delta}\frac{m}{\bar{r}_i}\left(\bar{u}_\theta-c_\theta\right)^2+\rho_g\hat{\delta}\frac{\bar{u}_\theta^2}{\bar{r}_i}\right] \tag{21}$$

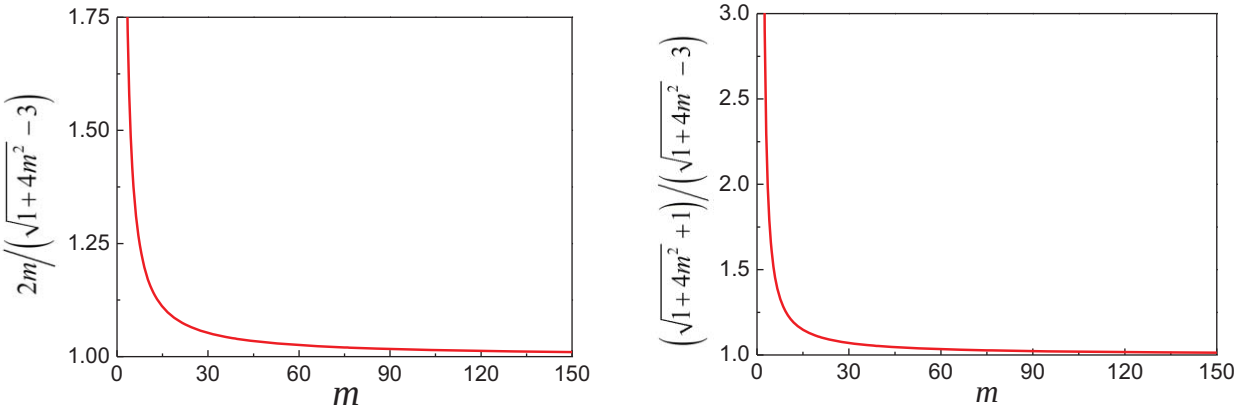

Figure 5. Dependence of the values of $2m\Big/\left(\sqrt{1+4m^2}-3\right)$ and $\left(\sqrt{1+4m^2}+1\right)\Big/\left(\sqrt{1+4m^2}-3\right)$ variation upon *m*.

Since the liquid film is infinite in the axial direction while it is periodic in the azimuthal direction, for the simplest case, we assume $k = m/\bar{r}_i$, then the total perturbed normal force $\hat{N}_{ig}$ exerted by the gas core in swirling annular flow acting on the interface can be obtained by applying the principle of superposition.

$$\hat{N}_{ig} = \left(\hat{N}_{ig}\right)_1 + \left(\hat{N}_{ig}\right)_2 = -\left[\rho_g \hat{\delta} k \left(\bar{u}_g - c\right)^2 + \rho_g \hat{\delta} \frac{\bar{u}_{g,\theta}^2}{\bar{r}_i}\right] \tag{22}$$

where

$$u^2 = u_z^2 + u_\theta^2, \qquad c^2 = c_z^2 + c_\theta^2 \tag{23}$$

In order to investigate the action of rotation on the interfacial stability, the swirl intensity is quantified in terms of number S_w, which is defined as the ratio of azimuthal velocity and mean velocity.

$$S_w = \sin\theta = \frac{u_\theta}{u} \tag{24}$$

Thus, if swirl intensity increases, number S_w increases, and vice versa.

Therefore, the overall normal stress (including both steady and disturbed ones) exerted by gas flow on the interface can be expressed as

$$N_{ig} = \bar{N}_{ig} + \hat{N}_{ig} e^{iks} = \bar{N}_{ig} - \left[\rho_g \hat{\delta} k \left(\bar{u}_g - c\right)^2 + \rho_g \hat{\delta} \frac{\left(S_w\right)^2 \bar{u}_g^2}{\bar{r}_i}\right] e^{iks} \tag{25}$$

where $\bar{N}_{ig}$ is the steady normal stress exerted by gas phase in swirling annular flow.

2.3. Liquid film analysis

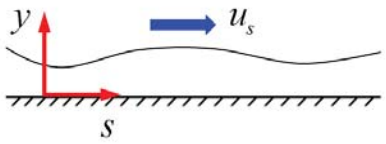

Figure 6. Liquid film flow in Cartesian coordinates.

A similar procedure can be used to drive an expression for the normal stress at the interface due to the liquid film in swirling annular flow. The film is considered to be sufficiently thin that the Cartesian coordinates can be used for this derivation (Fig. 6). Taking into account the effect of circular movement, the centrifugal force induced by the swirl is added as a source term in the momentum equation.

Then the equations of continuity and motion for two-dimensional Cartesian coordinates (y, s) are given as:

$$\begin{aligned}
&\frac{\partial u_y}{\partial y} + \frac{\partial u_s}{\partial s} = 0 \\
&u_y \frac{\partial u_y}{\partial y} + u_s \frac{\partial u_y}{\partial z} = -\frac{1}{\rho_l}\frac{\partial p}{\partial y} - \frac{u_\theta^2}{R_o - y} + \nu_l\left(\frac{\partial^2 u_y}{\partial y^2} + \frac{\partial^2 u_y}{\partial s^2}\right) \\
&u_y \frac{\partial u_s}{\partial y} + u_s \frac{\partial u_s}{\partial s} = -\frac{1}{\rho_l}\frac{\partial p}{\partial s} + \nu_l\left(\frac{\partial^2 u_s}{\partial y^2} + \frac{\partial^2 u_s}{\partial s^2}\right)
\end{aligned} \tag{26}$$

where variable $y = R_o - r$ and s denotes the streamwise direction.

The azimuthal velocity can be calculated as

$$u_\theta = u_s S_w \tag{27}$$

The equations for stream function and pressure in Cartesian coordinates are described as

$$\psi = \bar{\psi}(y) + \hat{\psi}(y)e^{iks}, \qquad p = \bar{p}(s) + \hat{p}(y)e^{iks} \tag{28}$$

The velocity components can be expressed as $u_y = -\partial\psi/\partial s$ and $u_s = \partial\psi/\partial y$.

Using a similar analysis procedure as the gas phase, the amplitude of the pressure perturbation can be expressed in terms of the film thickness ($\bar{\delta}$, $\hat{\delta}$), liquid density ρ_l, average film velocity $\bar{u}_l$, swirl intensity S_w, wavenumber k and wave velocity c as

$$\hat{p} = -\rho_l \hat{\delta}\bar{\delta}k^2(\bar{u}_l - c)^2 \frac{\dfrac{e^{n_1 y}-1}{n_1} - \dfrac{e^{n_2 y}-1}{n_2}}{\left(e^{n_1\bar{\delta}} - e^{n_2\bar{\delta}}\right)\bar{\delta}} - \frac{\rho_l\hat{\delta}\left(S_w\right)^2\bar{u}_l^2}{\bar{r}_i}\frac{e^{n_1 y}-e^{n_2 y}}{e^{n_1\bar{\delta}}-e^{n_2\bar{\delta}}} \tag{29}$$

where

$$n_1 = \frac{\dfrac{\left(S_w\right)^2}{\bar{r}_i} + \sqrt{\left[\dfrac{\left(S_w\right)^2}{\bar{r}_i}\right]^2 + 4k^2}}{2}, \qquad n_2 = \frac{\dfrac{\left(S_w\right)^2}{\bar{r}_i} - \sqrt{\left[\dfrac{\left(S_w\right)^2}{\bar{r}_i}\right]^2 + 4k^2}}{2} \tag{30}$$

The amplitude of the perturbed normal stress $\hat{N}_{il}$ exerted on the interface $y = \bar{\delta}$ as a result of the motion of liquid film is then given as

$$\hat{N}_{il} = \rho_l k^2\hat{\delta}\bar{\delta}(\bar{u}_l - c)^2 \frac{\dfrac{e^{n_1\bar{\delta}}-1}{n_1} - \dfrac{e^{n_2\bar{\delta}}-1}{n_2}}{\left(e^{n_1\bar{\delta}} - e^{n_2\bar{\delta}}\right)\bar{\delta}} - \frac{\rho_l\hat{\delta}\left(S_w\right)^2\bar{u}_l^2}{\bar{r}_i} \tag{31}$$

Fig. 7(a) and (b) shows how the ratio of $\left[\left(e^{n_1\bar{\delta}}-1\right)/n_1 - \left(e^{n_2\bar{\delta}}-1\right)/n_2\right]/\left(e^{n_1\bar{\delta}} - e^{n_2\bar{\delta}}\right)\bar{\delta}$ changes with the $k\bar{\delta}$. In this figure, two typical values of the cylinder radius R_o=10mm and R_o=20mm are selected for comparison and verification.

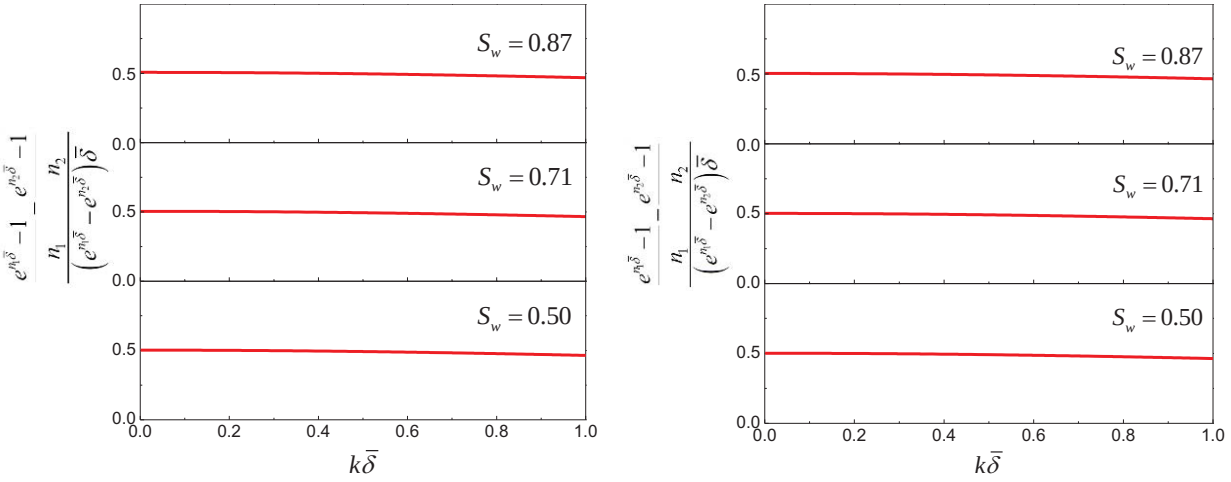

(a) R_o=10mm **(b) R_o=20mm**

Figure 7. Dependence of the value of $\left[\left(e^{n_1\bar{\delta}}-1\right)/n_1 - \left(e^{n_2\bar{\delta}}-1\right)/n_2\right]/\left(e^{n_1\bar{\delta}} - e^{n_2\bar{\delta}}\right)\bar{\delta}$ variation upon $k\bar{\delta}$.

The liquid film in swirling annular flow is very thin, which is in order of 0.1~1mm according to the experimental data of [1-4]. So for long waves $k\bar{\delta}$ will be very small and when $k\bar{\delta} < 1$, the value of

$\left[\left(e^{n_1\bar{\delta}}-1\right)/n_1-\left(e^{n_2\bar{\delta}}-1\right)/n_2\right]/\left(e^{n_1\bar{\delta}}-e^{n_2\bar{\delta}}\right)\bar{\delta}$ remains approximately 0.5, then the Eq. (31) can be simplified to

$$\hat{N}_{il}=\frac{\rho_l\hat{\delta}\bar{\delta}k^2}{2}\left(\bar{u}_l-c\right)^2-\frac{\rho_l\hat{\delta}\left(S_w\right)^2\bar{u}_l^2}{\bar{r}_i} \tag{32}$$

Therefore, the normal stress exerted by the liquid film on the interface is

$$N_{il}=\bar{N}_{il}+\hat{N}_{il}e^{iks}=\bar{N}_{il}+\left[\frac{\rho_l\hat{\delta}\bar{\delta}k^2}{2}\left(\bar{u}_l-c\right)^2-\frac{\rho_l\hat{\delta}\left(S_w\right)^2\bar{u}_l^2}{\bar{r}_i}\right]e^{iks} \tag{33}$$

where $\bar{N}_{il}$ is the steady normal stress exerted by liquid film in swirling annular flow.

2.4. Interfacial stability calculation (Dispersion relation)

The interfacial stability conditions for inviscid swirling annular flow can be found by balancing the normal stresses exerted by the gas and liquid phase (N_{ig}, N_{il}), and the stabilizing force of surface tension stress $\sigma\chi$ at the wavy interface. At the crest of the wave shown in Fig. 1, the stability equation is given by

$$N_{il}-N_{ig}=\sigma\chi \tag{34}$$

where χ and σ are the interface curvature and surface tension, respectively.

Since the balance of forces is done at the peak of the wave, the curvature is calculated at that point where it actually has its maximum value. This maximum curvature is calculated by Eq. (1) at s=0

$$\chi=k^2\hat{\delta}e^{iks} \tag{35}$$

Substituting Eqs. (25), (33) and (35) into (34) yields the following dispersion relation of the interfacial wave

$$\rho_l\left(\bar{u}_l-c\right)^2\frac{1}{2}k\bar{\delta}+\rho_g\left(\bar{u}_g-c\right)^2=k\sigma+\frac{\left(S_w\right)^2\left(\rho_l\bar{u}_l^2-\rho_g\bar{u}_g^2\right)}{\bar{r}_ik} \tag{36}$$

The above equation indicates that the extra terms deriving from circular movement of each phase have been introduced into the dispersive equation of the interfacial waves to account for the amplitude of the disturbance at the wavy interface. By solving this equation, the real and imaginary parts of the wave velocity can be expressed as

$$c_R=\frac{\frac{1}{2}k\bar{\delta}\rho_l\bar{u}_l+\rho_g\bar{u}_g}{\frac{1}{2}k\bar{\delta}\rho_l+\rho_g} \tag{37}$$

$$c_I=\frac{\left\{\frac{1}{2}\rho_l\rho_gk\bar{\delta}\left(\bar{u}_g-\bar{u}_l\right)^2-\left[k\sigma+\frac{\left(S_w\right)^2\left(\rho_l\bar{u}_l^2-\rho_g\bar{u}_g^2\right)}{\bar{r}_ik}\right]\left(\frac{1}{2}\rho_lk\bar{\delta}+\rho_g\right)\right\}^{\frac{1}{2}}}{\frac{1}{2}\rho_lk\bar{\delta}+\rho_g} \tag{38}$$

Following a temporal analysis, a necessary condition for the stability is c_I<0. Hence, the stability criterion is obtained, that is

$$\underbrace{k\sigma+\frac{\left(S_w\right)^2\left(\rho_l\bar{u}_l^2-\rho_g\bar{u}_g^2\right)}{\bar{r}_ik}}_{\text{stabilizing}}>\underbrace{\frac{\frac{1}{2}\rho_l\rho_gk\bar{\delta}\left(\bar{u}_g-\bar{u}_l\right)^2}{\frac{1}{2}\rho_lk\bar{\delta}+\rho_g}}_{\text{destabilizing}} \tag{39}$$

The above inequality will degenerate into the stability criterion for annular two-phase flow derived by [7] if the swirl intensity S_w which is related to the action of rotation equals zero.

3. Linear stability analysis

In order to study the influence of swirl intensity and the radius of cylinder on the stability of the film flow, geometry parameters and flow parameters of each phase selected for this study include (1) cylinder radius R_o: 10, 15 and 20mm; (2) swirl intensity S_w: 0, 0.5, 0.71, 0.87 (corresponding to the swirl angle θ: 0°, 30°, 45°, 60°); (3) mean gas velocity $\bar{u}_g$: 15~30m/s; (4) mean liquid velocity $\bar{u}_l$: 1.72m/s.

3.1. Amplitude growth rate

The value of c_I is the amplitude growth rate of the disturbance and is illustrated in Fig. 8 as a function of the wavelength λ, for a given flow condition and at various swirl intensity S_w and cylinder radius R_o. The average thickness of liquid film is 0.923mm in all cases. As the above discussion, if the growth rate remains less than zero for all wavelengths, any disturbed interfacial wave will decay over time, which means that the interface is always stable. However, if positive values for the growth rate exist, the flow will become unstable. As shown in Fig. 8(a), it is observed that at the same other conditions, the growth rate for disturbance in annular flow (S_w=0) is higher in comparison with those obtained for swirling flows (S_w>0). The addition of swirl both causes the disturbance to spiral as it travels downstream and the induced centrifugal force decays the amplitude of the disturbance. Namely, the wave produced in swirling condition grows slower than that in annular regime. Similarly, for a certain swirling annular flow, a smaller cylinder radius R_o results in a more stable flow as shown in Fig. 8(b).

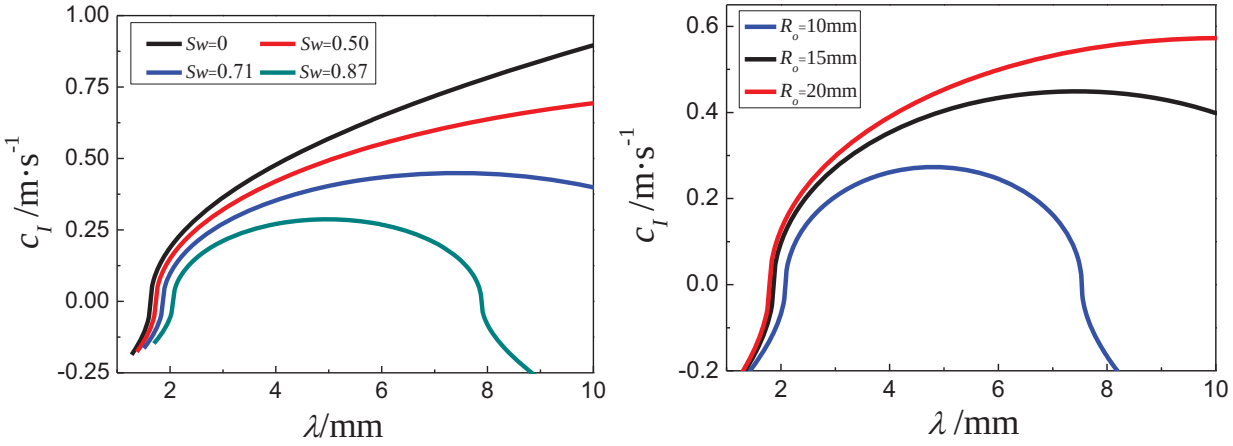

(a) **(b)**

Figure 8. Growth rate of disturbed waves at a film thickness of 0.923mm for various: (a)S_w values at u_g=17.0m/s, u_l=1.72m/s, R_o=15mm; (b)R_o values at u_g=17.0m/s, u_l=1.72m/s, S_w =0.71.

According to Eq. (35), the effect of the surface tension ($\sigma\chi$) on the interfacial stability depends on the wavelength λ: short wavelengths tend to stabilize the flow, whereas long wavelengths tend to destabilize it. The present analysis indicates that the existence of a critical wavelength λ_c for each curve within the small wavelength regime (λ<7mm), for which there is a balance between surface tension force, centrifugal force and gas-liquid relative flow. On this neutral stability condition, the amplitude of disturbance remains constant and does not change with time. In addition, Fig. 8(a) and (b) also indicates that for stronger swirl intensity and smaller cylinder radius, there is a small influence of surface tension on the stability region (c_I<0), because the stabilizing centrifugal force is dominant on this condition. However,

for lower swirl intensity and larger cylinder radius, the flow tends to become conditional stable, showing the importance of the surface tension acquires in this case.

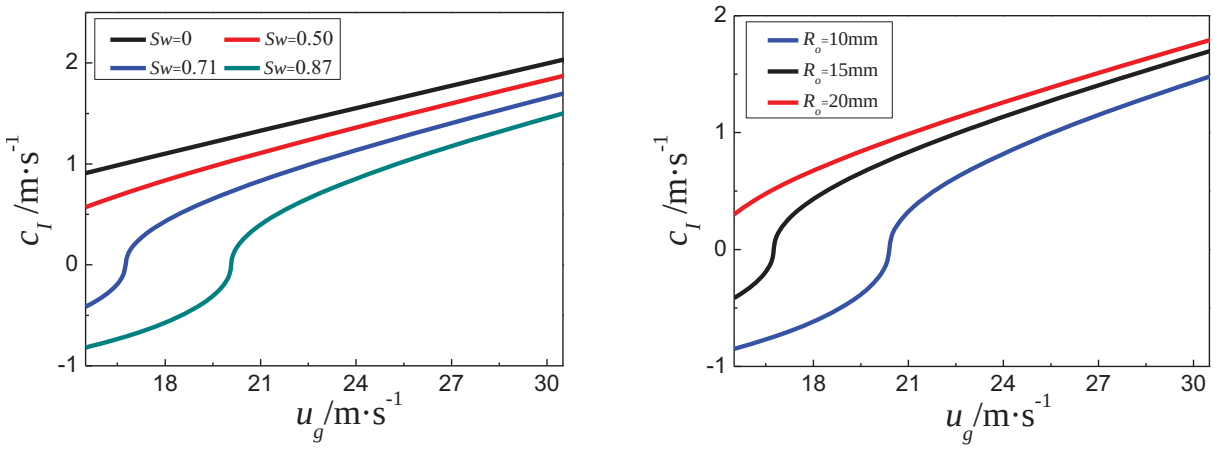

Figure 9. Growth rate of disturbed waves at a film thickness of 0.923mm for various (a)S_w values at u_l=1.72m/s, R_o=15mm, λ=10mm; (b) R_o values at u_l=1.72m/s, S_w=0.71, λ=10mm.

The amplitude growth rate c_I is illustrated in Fig. 9(a) and (b) as a function of gas mean velocity, for a constant liquid flow and at various swirl intensity S_w and cylinder radius R_o. The average thickness of liquid film is 0.923mm and wavelength is 10mm in all cases. Similar to above analysis, for a given flow condition, the growth rate c_I decreases as the value of S_w increases and R_o decreases, indicating that a larger swirl intensity results in a more stable flow, and the increased cylinder radius makes the film more unstable. From the figure, it is also noted that within a small gas flow rate region, the relative movement between the two phases is so small that for a strong swirl intensity or small cylinder radius in swirling flows, the combination of centrifugal force and surface tension force can prevail over the destabilizing relative motion of the two phases. On this condition, amplitudes of disturbance wave will decay and flow becomes stable.

3.2. Neutral stability curves

By setting c_I=0, the neutral stability curve can be easily determined from Eqs. (38). The λ_c-u_g plane is divided into two different characteristic regions by the neutral stability curve. One is the linearly stable region (c_I<0) where small disturbances decay with time and the other is the linearly unstable region (c_I>0) where the small disturbance grows as time increases.

The effect of swirl intensity S_w and cylinder radius R_o on the neutral curves for various gas flow conditions are shown in Fig. 10. As shown in Fig. 10(a), with the increase of swirl intensity, the critical value of wavelength λ_c increases and so the area of linearly stable region enlarges. Hence, it is concluded that the swirl motion implicates a stabilizing effect on the growth of disturbance. This swirl action induces additional centrifugal force acting as a "rigidity" to the wavy interface, decreasing the pressure gradient in the normal direction and making the interface stable. Fig. 10(b) shows the neutral stability curves of a swirling flow (S_w=0.71) with different values of cylinder radius R_o. The results indicate that the unstable region grows for an increasing R_o. Therefore, the cylinder radius has a destabilizing effect on the stability of the system. For a given flow condition, as cylinder radius increases, the centrifugal force acting on the wavy interface decreases. As a consequence of this, amplitudes of disturbance wave will grow and system becomes unstable. In addition, it can be found that the wavelength of neutral mode λ_c is very sensitive to the values of S_w and R_o when gas-liquid relative movement is small. However, when gas flowrate is large enough, there is not implicit difference in these values.

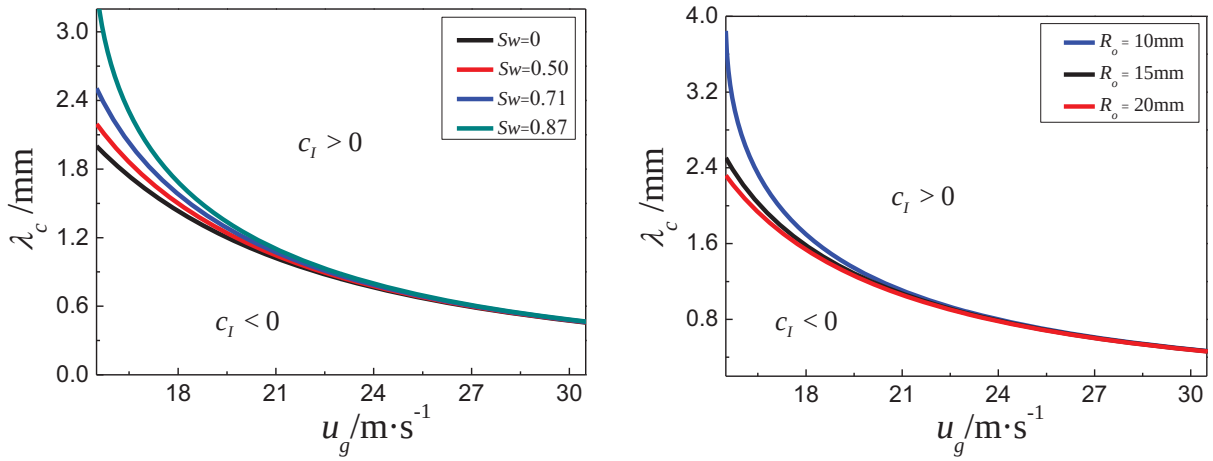

Figure 10. Neutral stability curves at a film thickness of 0.923mm for various (a)S_w values at u_l=1.72m/s, R_o=15mm; (b)R_o values at u_l=1.72m/s, S_w=0.71.

4. CONCLUSIONS

A three-dimensional linear temporal instability analysis has been carried out to model the interfacial stability of swirling annular flow. The swirling gas flow is deposited into a annular flow superposes a circular movement while the swirling liquid film flow is regard as two-dimensional flow. In the case of small disturbance, the interfacial stability criterion is obtained. The effects of the relative motion of gas-liquid flow, swirl intensity and cylinder radius on the interfacial stability are detailed investigated. From this study, we can draw the following conclusions:

(1) For a given flow condition, a cylinder with larger radius induces the flow instability condition while the stable region enlarges significantly by the existence of swirling motion;

(2) For a given flow condition with strong swirl intensity and small cylinder radius, there is a small influence of surface tension on the stability region whereas for lower swirl intensity and larger cylinder radius, the flow tends to become conditional stable, showing the importance of the surface tension acquires in this case;

(3) Under neutral stability conditions, the value of the critical wavelength is very sensitive to the swirl intensity and cylinder radius when gas-liquid relative movement is small. However, when gas flow-rate is large enough, there is no significant difference in its value.

APPENDIX

The equations of motion and continuity for circular movement of gas core are given in terms of plane polar coordinates

$$\begin{aligned}
&\frac{1}{r}\frac{\partial}{\partial r}\left(ru_r\right)+\frac{1}{r}\frac{\partial u_\theta}{\partial \theta}=0\\
&u_r\frac{\partial u_r}{\partial r}+\frac{u_\theta}{r}\frac{\partial u_r}{\partial \theta}-\frac{u_\theta^2}{r}=-\frac{1}{\rho_g}\frac{\partial p}{\partial r}+v_g\left[\nabla^2 u_r-\frac{u_r}{r^2}-\frac{2}{r^2}\frac{\partial u_\theta}{\partial \theta}\right]\\
&u_r\frac{\partial u_\theta}{\partial r}+\frac{u_\theta}{r}\frac{\partial u_\theta}{\partial \theta}+\frac{u_r u_\theta}{r}=-\frac{1}{\rho_g}\frac{\partial p}{r\partial \theta}+v_g\left[\nabla^2 u_\theta-\frac{u_\theta}{r^2}+\frac{2}{r^2}\frac{\partial u_r}{\partial \theta}\right]
\end{aligned} \tag{40}$$

By introducing the Stokes stream function ψ, the respective velocity components can be expressed as $u_r = \partial\psi / r\partial\theta$ and $u_\theta = -\partial\psi/\partial r$. The equations for stream function and pressure are expressed as

$$\psi = \bar{\psi}(r) + \hat{\psi}(r)e^{im\theta}, \qquad p = \bar{p}(\theta) + \hat{p}(r)e^{im\theta} \tag{41}$$

where *m* is the azimuthal wavenumber.

Substituting Eq. (41) into Eq. (40) and eliminating the steady-state solution, the equations governing disturbances are obtained

$$-\frac{m^2 u_\theta}{r^2}\hat{\psi} + \frac{u_\theta}{r}D\hat{\psi} = -\frac{D\hat{p}}{\rho_g}, \qquad \hat{\psi}Du_\theta - u_\theta D\hat{\psi} + \frac{u_\theta}{r}\hat{\psi} = -\frac{\hat{p}}{\rho_g} \tag{42}$$

Eliminating perturbed pressure $\hat{p}$ from above equations and assuming that viscous effects are negligible, the inviscid form of the Orr-Sommerfeld equation in polar coordinates is given as

$$(u_\theta - c_\theta)\left(D^2\hat{\psi} - \frac{m^2}{r^2}\hat{\psi}\right) + \hat{\psi}\left(\frac{u_\theta}{r^2} - D^2 u_\theta - \frac{Du_\theta}{r} - \right) = 0 \tag{43}$$

Since the gas flow is assumed to be inviscid, the motion of a given fluid element in rotating gas core is not influenced by the neighboring element at smaller and larger radii. The moment of momentum in gas core is conserved and the model of a potential vortex flow is considered. The azimuthal velocity distribution in such a flow can be expressed as

$$u_\theta = C/r \tag{44}$$

where *C* is a constant.

Substituting Eq. (44) to Eq. (43), the value of second term in left hand in Eq. (43) equals zero and this equation can be simplified to an Euler equation

$$D^2\hat{\psi} - \frac{m^2}{r^2}\hat{\psi} = 0 \tag{45}$$

with the general solution

$$\hat{\psi}(r) = Dr^{\frac{1+\sqrt{1+4m^2}}{2}} + Er^{\frac{1-\sqrt{1+4m^2}}{2}} \tag{46}$$

The *D* and *E* are constants depending on the boundary conditions at the axis and interface.

The radial velocity component can be calculated as

$$\hat{u}_r = \frac{1}{r}\frac{\partial\hat{\psi}}{\partial\theta} = \frac{\hat{\psi}}{r}ime^{im\theta} = \left(Dr^{\frac{\sqrt{1+4m^2}-1}{2}} + Er^{\frac{-\sqrt{1+4m^2}-1}{2}}\right)ime^{im\theta} \tag{47}$$

The boundary condition of radial velocity at the cylinder axis *r*=0 is given as

$$\hat{u}_r = 0 \tag{48}$$

The boundary condition of radial velocity at the perturbed interface r_i can be approximated according to the potential vortex flow in azimuthal direction as

$$\hat{u}_r = (\bar{u}_{g,\theta} - c)\frac{\partial r_i}{\bar{r}_i\partial\theta} \tag{49}$$

where $\bar{u}_{g,\theta} = C/\bar{r}_i$ is the average azimuthal velocity on the interface.

The radial position of the interface r_i in the azimuthal direction θ is

$$r_i = \left(R_o - \bar{\delta}\right) + \hat{\delta}e^{im\theta} \tag{50}$$

Then

$$\hat{u}_r = \hat{\delta}\frac{\left(\bar{u}_{g,\theta} - c_\theta\right)}{\bar{r}_i} ime^{im\theta} \tag{51}$$

where $\bar{\delta}$, $\hat{\delta}$, $\bar{u}_{g,\theta}$ and c_θ are the average and perturbed film thickness, average azimuthal velocity on the interface and azimuthal wave velocity, respectively.

Taking the above boundary conditions into account leads to the final expression for the perturbation of the stream function

$$\hat{\psi} = (\bar{u}_{g,\theta} - c_\theta)\hat{\delta}\left(\frac{r}{\bar{r}_i}\right)^{\frac{1+\sqrt{1+4m^2}}{2}} \tag{52}$$

Based on Eq.(52), the amplitude of the perturbed pressure can be derived from the integration of Eq.(42), which is related to the azimuthal velocity as

$$\hat{p}_{g2} = \left[\frac{\rho_g\hat{\delta}\left(\bar{u}_\theta - c_\theta\right)\left(u_\theta - c_\theta\right)}{\bar{r}_i}\frac{2m^2}{\sqrt{1+4m^2}-3} - \frac{\rho_g\hat{\delta}\bar{u}_\theta u_\theta}{\bar{r}_i}\frac{\sqrt{1+4m^2}+1}{\sqrt{1+4m^2}-3}\right]\left(\frac{r}{\bar{r}_i}\right)^{\frac{\sqrt{1+4m^2}-1}{2}} \tag{53}$$

ACKNOWLEDGMENTS

This work was financially supported by the National Nature Science Foundation of China under the Contract No. 51276140.

NOMENCLATURE

c	wave velocity (complex), m/s	c_R	phase velocity of wave, m/s
c_I	growth rate of wave, m/s	k	wavenumber in flow direction, m^{-1}
m	azimuthal wavenumber	r_i	radial position of interface, m
$\hat{y}$	disturbance amplitude, m^{-1}	σ	surface tension, N/m
χ	interface curvature, m^{-1}	δ	film thickness, m
S_w	swirl intensity	N_i	normal stress, Pa
I_0	zero-order modified Bessel function of first kind	I_1	first-order modified Bessel functions of first kind
K_1	first-order modified Bessel functions of second kind	A-E	constants

REFERENCES

1. H. Kataoka, A. Tomiyama, S. Hosokawa, A. Sou and M. Chaki, "Two-phase swirling flow in a gas–liquid separator," *Journal of Power and Energy Systems*. **2**(4), pp. 1120-1131 (2008).
2. H. Kataoka, Y. Shinkai, S. Hosokawa and A. Tomiyama, "Swirling annular flow in a steam separator," *Journal of Engineering for Gas Turbines and Power*. **131**(3), paper No. 032904, pp. 1-7 (2009a).
3. H. Kataoka, Y. Shinkai and A. Tomiyama, "Pressure drop in two-phase swirling flow in a steam separator," *Journal of Power and Energy Systems*. **3**(2), pp. 382-392 (2009b).
4. H. Kataoka, Y. Shinkai and A. Tomiyama, "Effects of swirler shape on two-phase swirling flow in a steam separator," *Journal of Power and Energy Systems*. **3**(2), pp. 347-355 (2009c).
5. R. Molina, S. Wang, L.E. Gomez, R.S. Mohan, O. Shoham and G. Kouba, "Wet Gas Separation in Gas-Liquid Cylindrical Cyclone Separator," *Journal of Energy Resources Technology*. **130**(4), paper No. 042701, pp. 1-13 (2008).

6. P.J. Fryer and P.B. Whalley, "The effect of swirl on the liquid distribution in annular two-phase flow," *International Journal of Multiphase Flow*. **8**(3), pp. 285-289 (1982).
7. G. Hewitt and N. Hall-Taylor, *Annular Two-Phase Flow*, pp. 100, Pergamon Press, New York (1970).
8. D.E. Woodmansee and T.J Hanratty, "Mechanism for the removal of droplets from a liquid surface by a parallel air flow," *Chemical Engineering Science*. **24**(2), pp. 299-307 (1969).
9. D.E. Woodmansee, "Atomization from a Flowing Horizontal Water Film by a Parallel Air Flow," Ph.D. Thesis in Chem. Eng., University of Illinois (1968).
10. G.I. Taylor, "Generation of Ripples by Wind Blowing over a Viscous Fluid," The Scientific Papers of Sir G.I. Taylor, Ⅲ(Edicated by G.K. Batchelor), 244, Cambride University Press (1963).
11. D.F. Tatterson, "Rates of atomization and drop size in annular two-phase flow," Ph.D. Thesis, University of Illinois, Urbana (1975).
12. J.L. Trallero, "Oil-water flow patterns in horizontal pipes," ph.D. Thesis, University of Tulsa (1995).
13. T. Al-Wahaibi and P. Angeli, "Transition between stratified and non-stratified horizontal oul-water flows. Part 1: Stability analysis," *Chemical Engineering Science*. **62**(11), pp. 2915-2928 (2007).
14. M.J. Holowach, L.E. Hochreiter and F.B. Cheung, "A model for droplet entrainment in heated annular flow," *International Journal of Heat and Fluid Flow*. **23**(6), pp. 807–822 (2002).
15. S.H. Ryua and G.C. Park, "A droplet entrainment model based on the force balance of an interfacial wave in two-phase annular flow," *Nuclear Engneering and Design*, **241**(9), pp. 3890–3897 (2011).
16. L.A. Dávalos-Orozco, G. Ruiz- Chavarría, "Hydrodynamic instability of a fluid layer flowing down a rotating cylinder", *Physics of Fluids A: Fluid Dynamics*, **5**(10), pp. 2390-2404 (1993).
17. G. Ruiz- Chavarría, L.A. Dávalos-Orozco, "Azimuthal and streamwise disturbances in a fluid layer flowing down a rotating cylinder", *Physics of Fluids*, **9**(10), pp. 2899-2908 (1997).
18. L.A. Dávalos-Orozco, E. Vázquez-Luis, "Instability of the interface between two inviscid fluids inside a rotating annulus in the absence of gravity", *Physics of Fluids*, **15**(9), pp. 2728-2739 (2003).
19. C.I. Chen, C.K. Chen, Y.T. Yang, "Weakly nonlinear stability analysis of thin viscoelastic film flowing down on the outer surface of a rotating vertical cylinder", *International journal of engineering science*, **41**(12), pp. 1313-1336 (2003).
20. C.I. Chen, "Non-linear stability characterization of the thin micropolar liquid film flowing down the inner surface of a rotating vertical cylinder", *Communications in Nonlinear Science and Numerical Simulation*, **12**(5), pp. 760-775 (2007).
21. G. Coppola, O. Semeraro, "Interfacial instability of two rotating viscous immiscible fluids in a cylinder", *Physics of Fluids*, **23**(6), pp. 334-339 (2011).
22. J.P. Matas, M. Hong, A. Cartellier, "Stability of a swirled liquid film entrained by a fast gas stream", *Physics of Fluids*, **26**(4), pp. 90-96 (2014).
23. M.V. Panchagnula, P.E. Sojka, P.J. Santangelo, "On the three-dimensional instability of a swirling, annular, inviscid liquid sheet subject to unequal gas velocities", *Physics of Fluids*, **8**(12), pp. 3300-3312 (1996).
24. K. Wang, B. Bai, W. Ma, "A model for droplet entrainment in churn flow," *Chemical Engineering Science*, **104**(50), pp. 1045-1055 (2013).